J. theor. Biol. (1995) **174,** 137–148

A Model for Glycolytic Oscillations based on Skeletal Muscle Phosphofructokinase Kinetics

PAUL SMOLEN†

Mathematical Research Branch, NIDDK, NIH, Bethesda, MD 20892, *U.S.A.*

(*Received on* 23 *March* 1994, *Accepted in revised form on* 30 *November* 1994)

Existing models for glycolytic oscillations are not based on detailed experimental kinetics of the glycolytic enzymes. Here, a model is constructed to fit the kinetics of skeletal muscle phosphofructokinase with respect to variations in AMP, ATP, fructose-6-P, and fructose 1,6-P_2 levels. A Monod–Wyman–Changeux model for a tetrameric enzyme is considered. However, it is found that the kinetic data fit considerably better with an assumption of identical, independent subunits. With parameters that fit these data and with a previous model for the rest of glycolysis, product activation of phosphofructokinase leads to oscillations of glycolytic intermediates and [ATP] resembling those observed experimentally in muscle extracts. The period is several minutes. The model can also produce oscillations at neutral pH and with [ATP] representative of an intact cell. Under both conditions the mean concentrations and oscillations vary with the rate of glucose phosphorylation in a plausible manner only if some amount of glucose-6-phosphatase or glucose-6-P dehydrogenase activity is assumed or if hexokinase is inhibited by glucose-6-P. Also, the model can be reduced to two variables for ease of analysis and the oscillation mechanism thereby illustrated.

1. Introduction

It is well known that the rate of glycolysis, and the concentrations of glycolytic intermediates, oscillate with a period of minutes (Hess & Boiteaux, 1971; Richter & Ross, 1981; Mathews & van Holde, 1990). The kinetics of glycolysis have been extensively studied in skeletal muscle extract (Tornheim & Lowenstein, 1973; Tornheim & Lowenstein, 1975; Tornheim & Lowenstein, 1976). Several mathematical models (Goldbeter & Lefever, 1972; Tornheim, 1979; Termonia & Ross, 1981; Markus & Hess, 1984) have been developed to explain glycolytic oscillations. All of these models rely on product activation of the enzyme catalyzing the third step in glycolysis, phosphofructokinase (PFK), to provide the positive feedback required for oscillations. The majority of the modeling work (Goldbeter & Lefever, 1972; Markus & Hess, 1984) applies more to glycolysis in yeast than in muscle, in that the authors use product activation by ADP rather than by fructose 1-6-P_2 (FBP).

The early model by Tornheim (1979) reproduces the oscillations in skeletal muscle extract reasonably well. It contains simple expressions for the rates of PFK and glyceraldehyde 3-P dehydrogenase (GPDH). The rate of PFK is assumed to depend on AMP, FBP, and F6P concentrations but in a primitive manner. In particular the dependence on [FBP] is discontinuous. The model is empirical, rather than derived from a theory of enzyme structure. Another model, perhaps the most widely used (Goldbeter & Lefever, 1972; Markus & Hess, 1984), is based on Monod–Wyman–Changeux (MWC) (Monod *et al.*, 1965; Cantor & Schimmel, 1980) concerted transition theory for two subunits—later extended to more subunits (Venieratos & Goldbeter, 1979). This MWC model only considers the effects of substrate (fructose-6-P or F6P) and product (ADP), and not other effectors such as ATP. Although PFK parameters in this model have an experimental basis, they are for a different organism (*E. coli*) than that where the oscillations modeled occur (yeast).

† Address for correspondence: Dr. Paul Smolen, Born Bunge Foundation, University of Antwerp-UIA, Universiteitsplein 1, B2610 Antwerp, Belgium. E-mail:smolen@kuifje.bbf.uia.dc.be

0022–5193/95/100137+12 $08.00/0

Another model (Termonia & Ross, 1981*a*, *b*) contains detailed expressions for the rates of PFK and pyruvate kinase, also based on MWC theory. However, the activation of PFK by FBP is not included, and parameters for this model are obtained from many sources as opposed to one defined system. Finally, simulations by Hess and colleagues (Boiteaux *et al*., 1975; Markus & Hess, 1984 used essentially the model of Goldbeter & Lefever (1972) for PFK and often superimposed a forced oscillation in glucose input rate. Only the early model of Tornheim (1979) incorporates mammalian PFK kinetics.

There is clearly a need for a more detailed model based on the kinetics of mammalian enzymes in a defined preparation where glycolytic oscillations occur. However, a comprehensive model for all the enzymes is difficult to produce because of complexity and particularly because detailed experimental data for all enzyme rates in such a preparation have not been assembled. However, such data exist for the velocity of rat skeletal muscle PFK (Tornheim & Lowenstein, 1976) purified from extract, and as noted above, PFK is generally thought to play a key role in generating oscillations. Thus, there is justification constructing a model that only treats PFK in detail.

The velocity of muscle PFK depends on many effectors. The dependencies on AMP, ATP, the substrate F6P, and the product FBP have been well characterized in Tornheim & Lowenstein (1976). Physiologically, the inhibitor citrate and the activators ADP and inorganic phosphate (Passoneau & Lowry, 1962; Parmeggiani & Bowman, 1963; Bloxham & Lardy, 1975) and fructose 2,6-P_2 (in liver, not muscle) (Tornheim, 1988) are probably also significant. But the dependence on these effectors is not well characterized and it is necessary to avoid excessive complexity, so these effectors are neglected here. The dependence on [F6P] is sigmoidal, as is the inhibition by [ATP] (Uyeda & Racker, 1965). In Tornheim & Lowenstein (1976) ATP is always saturating as a substrate ($K_m$ca.30 μM; Ling & Lardy, 1954). The dependencies on [FBP] and [AMP] appear hyperbolic.

The data of Tornheim & Lowenstein (1976) were compared with those of other authors. A Michaelis constant of 0.4 mM (Passoneau & Lowry, 1962) is reported for F6P in the presence of 2.3 mM ATP, pH 7, which is consistent with Tornheim & Lowenstein (1976) if allowance is made for the different [ATP]. The sigmoidicity of the velocity vs. [F6P] relation is enhanced by inhibitors (Koppelschlager *et al*., 1968) and reduced by activators (Bloxham & Lardy, 1975). The low K_a for AMP activation reported in Tornheim & Lowenstein (1976) appears to occur with high inorganic phosphate (Passoneau & Lowry, 1962). Finally, increasing [FBP] has been reported to increase K_i for ATP (Passoneau & Lowry, 1962). Thus, the dataset of Tornheim & Lowenstein (1976) is generally consistent with other studies. Because of its comprehensive nature it is used exclusively for the model fitting herein.

Because the active form of skeletal muscle PFK is predominantly tetrameric (Parmeggiani *et al*., 1966; Mathews & van Holde, 1990) it seems natural to use either an MWC concerted model, or a sequential model, to describe its allostery. There is considerable evidence that an MWC model cannot describe well the kinetics of PFK (see Discussion). However, such a model was tried as this type of model is so widely used.

To avoid great complexity, the velocity as a function of [ATP], [AMP], [F6P] and [FBP] did not explicitly include heterotropic interactions between ligands. Experimentally, increased [F6P] appears to tighten the binding of both FBP and AMP, and increased [AMP], [F6P] or [FBP] counteracts ATP inhibition. It was thought that effects of ligands upon the equilibrium between R and T states in an MWC model might suffice to reproduce these observations. But, this was found not to be the case.

However, it is shown here that a simple model—that of identical *independent* subunits with explicit heterotropic binding interactions between ligands—fits the data considerably better than the MWC model. Although the fit is still not very precise, it is qualitatively correct.

This PFK model is combined with a basic model of glycolysis first proposed by Tornheim (1979). Oscillations similar to those in extract are obtained. Also, oscillations are obtained under conditions of pH and total adenine nucleotide concentration similar to those in an intact cell. The model can then be reduced to two variables for a phase-plane analysis of the oscillations. This analysis in particular makes it evident that product activation by FBP is central to the oscillatory mechanism of muscle PFK.

Implications of this model—the first model of glycolytic oscillations based on a fit of detailed mammalian PFK kinetics—for slow (timescale of minutes) oscillations of [ATP] and related quantities observed in intact mammalian cells such as pancreatic β-cells or cardiac myocytes, are discussed.

2. Models and Methods

2.1. THE INDEPENDENT-SUBUNIT MODEL FOR PFK

Cumulative evidence, reviewed in Uyeda (1991), suggests that the muscle PFK reaction (in rabbit, and presumably rat) is well described as a steady-state Random Bi Bi mechanism with a central ternary

complex. In general, the velocity expression for this mechanism is extremely complex (Segel, 1975). However, in glycolysis the reverse reaction of PFK is very unfavorable energetically. Also, *in vitro* with varying [ATP] and [F6P], the forward reaction has been fit well with a much simpler velocity expression (Hanson *et al*., 1973), of the form appropriate for a rapid equilibrium random bimolecular reaction,

$$V=\frac{V_{\max}[\mathrm{ATP}][\mathrm{F6P}]}{K_{\mathrm{d,ATP}}K_{\mathrm{m,ATP}}+K_{\mathrm{m,ATP}}[\mathrm{ATP}]+K_{\mathrm{m,F6P}}[\mathrm{F6P}]+K_{\mathrm{m,ATP}}K_{\mathrm{m,F6P}}[\mathrm{ATP}][\mathrm{F6P}]}. \quad (1)$$

If [ATP] is much greater than its dissociation or Michaelis constants, as in the cases considered here, and if we neglect the reverse reaction, the velocity reduces to

$$V=\frac{V_{\max}[\mathrm{F6P}]}{K_{\mathrm{m,F6P}}+[\mathrm{F6P}]} \quad (2)$$

or steady-state, unireactant Michaelis–Menten kinetics.

$K_{\mathrm{m,F6P}}=K_{\mathrm{d,F6P}}$ would be rapid equilibrium kinetics. Although this was suggested for PFK *in vitro* (Kee & Griffen, 1972), more recent work suggests that $K_{\mathrm{d,F6P}}$ is about 20–30% of $K_{\mathrm{m,F6P}}$ (Bar-Tana & Cleland, 1974). However, for the current study, rapid equilibrium seems a reasonable assumption for the following reasons:

(i) Models using the rapid equilibrium assumption have fit velocity data for rabbit muscle PFK (Pettigrew & Frieden, 1979; (Waser *et al*., 1983) and *Plasmodium berghei* PFK (Buckwitz *et al*., 1988) rather well.

(ii) If rapid equilibrium is not assumed, modeling the kinetics of enzyme subject to multiple effectors is very difficult, and it is advantageous if data can be fitted by a model with fewer adjustable parameters, whose derivation can be readily understood.

With identical, independent subunits only one subunit needs consideration. It can bind, or not bind, AMP, FBP and F6P. Also, there are two sites (in addition to the catalytic site) where ATP can bind (Kemp & Krebs, 1967); both sites need to be inhibitory to give sufficiently steep ATP inhibition. ATP as substrate is always saturating so will not be explicitly considered. Then the subunit has $2^5=32$ possible states. The state with AMP, FBP and F6P bound and ATP not bound should be the most active. The velocity of PFK is proportional to the fraction of PFK in the active state. Assuming rapid equilibrium, this fraction is determined entirely by binding kinetics.

We denote AMP by L_1 and let it bind with dissociation constant K_1 when nothing else is bound, similarly let L_2 and K_2 correspond to FBP, L_3 and K_3 to F6P, and L_4 and K_4, K_5 to ATP with two binding sites. There are six heterotropic interactions. These are: binding L_1 multiplies K_3 by $f_{13}<1$ (AMP activation by tightening binding of F6P); binding L_2 multiplies K_3 by $f_{23}<1$ (FBP activation by tightening binding of F6P); binding L_4 multiplies K_1 by $f_{41}>1$ (ATP inhibition by weakening binding of AMP); binding L_4 multiplies K_2 by $f_{42}>1$ (ATP inhibition by weakening binding of FBP); and binding L_4 multiplies K_3 by $f_{43}>1$ at one ATP site and $f_{53}>1$ at the other (ATP inhibition by weakening binding of F6P). By elementary thermodynamics, each interaction implies its converse such that if binding L_i multiplies K_j binding L_j must identically multiply K_i. A state of the subunit is denoted $(\alpha\beta\gamma\delta\epsilon)$, where α is 0 if L_1 is not bound and 1 if L_1 is bound, etc, with δ and ϵ for the two ATP sites. The most active state of PFK is (11100). The 15 other states with F6P bound are each assumed to have the same "basal" specific activity whose ratio to that of (11100) is $\lambda \ll 1$. Let the fraction of PFK in state $(\alpha\beta\gamma\delta\epsilon)$ be denoted $w_{\alpha\beta\gamma\delta\epsilon}$. Then the velocity is

$$R_{\mathrm{PFK}}=V_{\max}\left[\frac{w_{11100}+\lambda(\Sigma_{\alpha\beta\delta\epsilon}w_{\alpha\beta1\delta\epsilon}-w_{11100})}{\Sigma_{\alpha\beta\gamma\delta\epsilon}w_{\alpha\beta\gamma\delta\epsilon}}\right]. \quad (3)$$

To calculate the velocity one first divides top and bottom by w_{00000},

$$R_{\mathrm{PFK}}=V_{\max}\left[\frac{\frac{w_{11000}}{w_{00000}}+\lambda\left(\Sigma_{\alpha\beta\delta\epsilon}\frac{w_{\alpha\beta1\delta\epsilon}}{w_{00000}}-\frac{w_{11100}}{w_{00000}}\right)}{\Sigma_{\alpha\beta\gamma\delta\epsilon}\frac{\omega_{\alpha\beta\gamma\delta\epsilon}}{w_{00000}}}\right]. \quad (4)$$

The ratio $w_{\alpha\beta\gamma\delta\epsilon}/w_{00000}$ is also the ratio of the concentration of PFK in state $(\alpha\beta\gamma\delta\epsilon)$ to concentration of PFK in state (00000). These ratios can be computed from ligand concentrations and dissociation constants. For example, almost immediately from definition,

$$K_1=\frac{w_{00000}[L_1]}{w_{10000}} \quad (5)$$

$$K_2=\frac{w_{10000}[L_2]}{w_{11000}} \quad (6)$$

$$f_{13}f_{23}K_3=\frac{w_{11000}[L_3]}{w_{11100}}. \quad (7)$$

To obtain the last of these it is assumed that when several ligands are bound, heterotropic interactions multiply together (their free energies add). From these expressions one obtains successively.

$$\frac{w_{10000}}{w_{00000}}=\frac{[L_1]}{K_1} \tag{8}$$

$$\frac{w_{11000}}{w_{00000}}=\frac{[L_1]}{K_1}\frac{[L_2]}{K_2} \tag{9}$$

$$\frac{w_{11100}}{w_{00000}}=\frac{[L_1]}{K_1}\frac{[L_2]}{K_2}\frac{[L_3]}{f_{13}f_{23}K_3}. \tag{10}$$

The velocity of PFK often depends sigmoidally on [F6P] (L_3). To incorporate this semiempirically, a Hill coefficient of 2 is assumed henceforth to describe F6P binding. Then eqn (7) is modified slightly,

$$f_{13}f_{23}K_3=\frac{w_{11000}[L_3^2]}{w_{11100}} \tag{11}$$

as in eqn (10).

All ratios can be similarly obtained and a generalized expression, suitable for programming, is obtained. Since $x^0=1$ for $x>0$,

$$\frac{w_{\alpha\beta\gamma\delta\epsilon}}{w_{00000}}=\frac{1}{(f_{13})^{\alpha\gamma}(f_{23})^{\beta\gamma}(f_{41})^{\delta\alpha}(f_{42})^{\delta\beta}(f_{43})^{\delta\gamma}(f_{53})^{\epsilon\gamma}} \times\frac{[L_1]^\alpha}{(K_1)^\alpha}\frac{[L_2]^\beta}{(K_2)^\beta}\frac{[L_3]^{2\gamma}}{(K_3)^\gamma}\frac{[L_4]^\delta}{(K_4)^\delta}\frac{[L_4]^\epsilon}{(K_5)^\epsilon} \tag{12}$$

From eqns (12) and (3) the rate of PFK can be obtained.

2.2. MWC MODEL

The assumptions are as follows: tetrameric PFK is either in the "R" or "T" state and the catalytic rate constant differs for each state; the subunits can bind only one each of AMP, ATP as substrate, F6P, FBP, or inhibitory ATP; dissociation constants differ between states but there are no heterotropic interactions between ligands; and only subunits with FBP, ATP, AMP and F6P bound and inhibitory ATP not bound are catalytically active. Let L be the ratio of [T] to [R] in the absence of ligands and k_T and k_R be the catalytic rate constants. For ligand i, with concentration C_i and dissociation constant K_i, define $\bar{K}_i=c_i/K_i$ and also subscript with R or T. Take inhibitory ATP as ligand 5. Rapid equilibrium is assumed to hold for ATP and F6P kinetics, and the reverse reaction neglected. These assumptions determine

$$R_{\mathrm{PFK}}=\frac{k_{\mathrm{T}}L\left[\prod_{i=1}^{4}\bar{K}_{i\mathrm{T}}(1+\bar{K}_{i\mathrm{T}})^3\right](1+\bar{K}_{5\mathrm{T}})^3 +k_{\mathrm{R}}\left[\prod_{i=1}^{4}\bar{K}_{i\mathrm{R}}(1+\bar{K}_{i\mathrm{R}})^3\right](1+\bar{K}_{5\mathrm{R}})^3}{L\prod_{i=1}^{5}(1+\bar{K}_{i\mathrm{T}})^4+\prod_{i=1}^{5}(1+\bar{K}_{i\mathrm{R}})^4} \tag{13}$$

The case of two inhibitory ATP sites was also tried.

2.3. DATA FITTING

For both the MWC and independent-subunit models of PFK, programs were written that automatically generated PFK rates for the conditions of the first five figures of (Tornheim & Lowenstein, 1976). For comparison, the experimental figures were scanned and their data digitized. Variation of parameters was first done by trial and error, to obtain a reasonable fit between experimental points and theoretical curves. Then parameters were further optimized by use of the International Mathematical and Statistical Library minimization subroutine UMINF (IMSL, 1991), which uses a method of steepest descent to minimize the sum of squared differences between the experimental and theoretical points.

2.4. GLYCOLYTIC OSCILLATIONS

To construct a model of glycolytic oscillations, Tornheim (1979) is followed. Hexokinase operates at a constant rate HK and glucose-6-P and F6P are in equilibrium with [F6P]/[glucose-6-P] $=K_{\mathrm{gf}}$. The reactions catalyzed by aldolase and triose phosphate isomerase always remain near equilibrium so that the concentration of dihydroxyacetone phosphate (DHAP) is proportional to $\sqrt{[\mathrm{FBP}]}$. The rate of glyceraldehyde 3-phosphate dehydrogenase, R_{GPDH}, is first-order with respect to [DHAP]. The GDPH reaction is assumed rate-limiting for following steps. ATP is produced in glycolysis with 2 net ATPs formed per glucose utilized, and degraded by an unspecified ATPase. The relations

$$[\mathrm{ATP}]+[\mathrm{ADP}]+[\mathrm{AMP}]=A_{\mathrm{tot}} \tag{14}$$

$$\frac{[\mathrm{ATP}][\mathrm{AMP}]}{[\mathrm{ADP}]^2}=K_{\mathrm{A}} \tag{15}$$

are assumed to hold, giving [AMP] and [ADP] if [ATP] is known.

These assumptions give a model with three dependent variables: [ATP], [F6P], and [FBP]:

$$\frac{\mathrm{d[ATP]}}{\mathrm{d}t} = -HK - R_{\mathrm{PFK}} - R_{\mathrm{ATPase}} + 2R_{\mathrm{GPDH}} \quad (16)$$

$$\frac{\mathrm{d[F6P]}}{\mathrm{d}t} = \frac{K_{\mathrm{gf}}}{1+K_{\mathrm{gf}}}(HK - R_{\mathrm{PFK}}) \quad (17)$$

$$\frac{\mathrm{d[FBP]}}{\mathrm{d}t} = R_{\mathrm{PFK}} - \tfrac{1}{2}R_{\mathrm{GPDH}} \quad (18)$$

with R_{PFK} as given above,

$$R_{\mathrm{ATPase}} = k_{\mathrm{ATP}}[\mathrm{ATP}], \quad (19)$$

and

$$R_{\mathrm{GPDH}} = k_{\mathrm{GPDH}}\sqrt{\frac{[\mathrm{FBP}]}{1\ \mu\mathrm{M}}}\left[\frac{\mathrm{ADP}}{K_{\mathrm{D}}+\mathrm{ADP}}\right] \quad (20)$$

This last expression is modified from Tornheim (1979) by adding a Michaelis–Menten term for [ADP].

Numerical integration was done with the Gear algorithm (Gear, 1967) as implemented in the LSODE package (Hindmarsh, 1974), and phase-plane analysis was done with the programs PhasePlane (Ermentrout, 1990) or AUTO (Doedel, 1981).

3. Results

3.1. FITTING VELOCITY DATA FOR PHOSPHOFRUCTOKINASE

In Tornheim & Lowenstein (1976) an extensive series of PFK rate measurements for different combinations of [F6P], [AMP], [ATP], and [FBP] values is presented, with data taken at pH 6.65, typical for oscillations in muscle extract, and at pH 7, at which ATP inhibition is shifted to higher [ATP].

Figure 1 shows one attempt to fit the pH 6.65 data using the MWC model. Here, symbols are experimental points and lines are theoretical curves. The fit is very poor—primarily because there are essentially no heterotropic interactions between ligands evident in the fit, in particular increased [AMP] does not effectively counter ATP inhibition and increased [F6P] does not significantly tighten the binding of AMP or FBP (i.e. the velocity curves for different [AMP] or [FBP] do not approach each other at high [F6P]).

However, Fig. 2 shows a fit using the independent-subunit model. In this model, increased [F6P] tightens the binding of AMP and FBP and also inhibits the binding of ATP, and all three of these interactions are required to fit qualitatively the data in figure 3 of Tornheim & Lowenstein (1976). Furthermore, the data in their figure 2 can only be fit if increased [AMP] and [FBP] inhibit—and thus shift to the right—the binding of ATP.

Panels (a)–(c) of Fig. 2 fit data taken at pH 6.65, and panels (d)–(e) fit data taken at pH 7, thus two sets of parameters are given, one for each pH. Dissociation constants for AMP, F6P, and ATP, in each case without other ligands present, have previously been estimated by gel filtration (Kemp & Krebs, 1967). Here, to obtain acceptable data fits, values for the constants are used which are of the same order as these estimates, but not identical.

The pH 6.65 fits [panels (a)–(c)] are qualitatively correct for shapes of curves and directions and scale of effects, but individual points are not always well approximated. The rate of PFK at low [FBP] [panel (b), 0.3 μM FBP] is overestimated. This may be evidence of cooperativity among subunits, in that the rate may fall off with a power of [FBP] > 1. The rate of PFK at high [AMP] [panel (a)] is underestimated. Also, it is evident from the experimental data in panel (c) that there is greater sigmoidicity of R_{PFK} vs. [F6P] at low [AMP] or [FBP]. This agrees with Bloxham & Lardy (1975) but is not fully captured by the model. The pH 7 fit [panels (d)–(e)] differs from the pH 7 data mainly in that the experimental [ATP] inhibition increases more rapidly than the model predicts [panel (d)]. ATP inhibition is shifted to higher [ATP] at pH 7 [comparing panels (b) and (d)]. Using higher, or variable, powers of all ligand concentrations would allow more exact fits. However, the model could not then be derived without many *ad hoc* assumptions.

For panels (a)–(c), the square root of the average squared difference between experimental and theoretical rates, or RMS error, is 0.378 μM min^{-1}; for panels (d)–(e) it is 0.270 μM min^{-1}. These RMS errors are respectively 20.6% and 18.5% of the average experimental rate of their datasets—these are significant errors, but can be largely interpreted as in the above paragraph. The sensitivity of fit S can be defined for parameter p and RMS error E as;

$$S = \frac{p\Delta E}{E\Delta p}.$$

For fractional $\Delta p (= \Delta p/p)$of 10% in panels (a)–(c), this varies from 8.0×10^{-7} for f_{41} to 2.06 for V_{max}. All parameters except V_{max} have S less than 1. Therefore, the fit is not very sensitive to any individual parameter. If we take a fractional Δp of 50%, all parameters except f_{41}, f_{43}, and f_{53} have $S > 0.35$, but these three parameters have $S < 0.003$. These three parameters are not well determined by the data, as long

as they are kept large ($>10^3$) the fit is little changed by varying them.

The fits depend very little on the "basal" PFK rate parameter λ for $\lambda <$ ca. 0.07.

3.2. MODELING GLYCOLYTIC OSCILLATIONS

The independent-subunit model of PFK was assigned parameters which fit the pH 6.65 data and combined with a simple model of glycolysis, as discussed in Modeling and Methods. With reasonable values for other enzymatic rate constants, oscillations in the glycolytic rate and the concentrations of ATP, F6P and FBP result. They are stable with respect to variations in initial concentrations. However, the average value of [F6P] during oscillations is very sensitive to variations in the hexokinase rate *HK*. To understand this, consider that the average PFK rate must equal *HK*. If *HK* drops slightly, [F6P] will drop

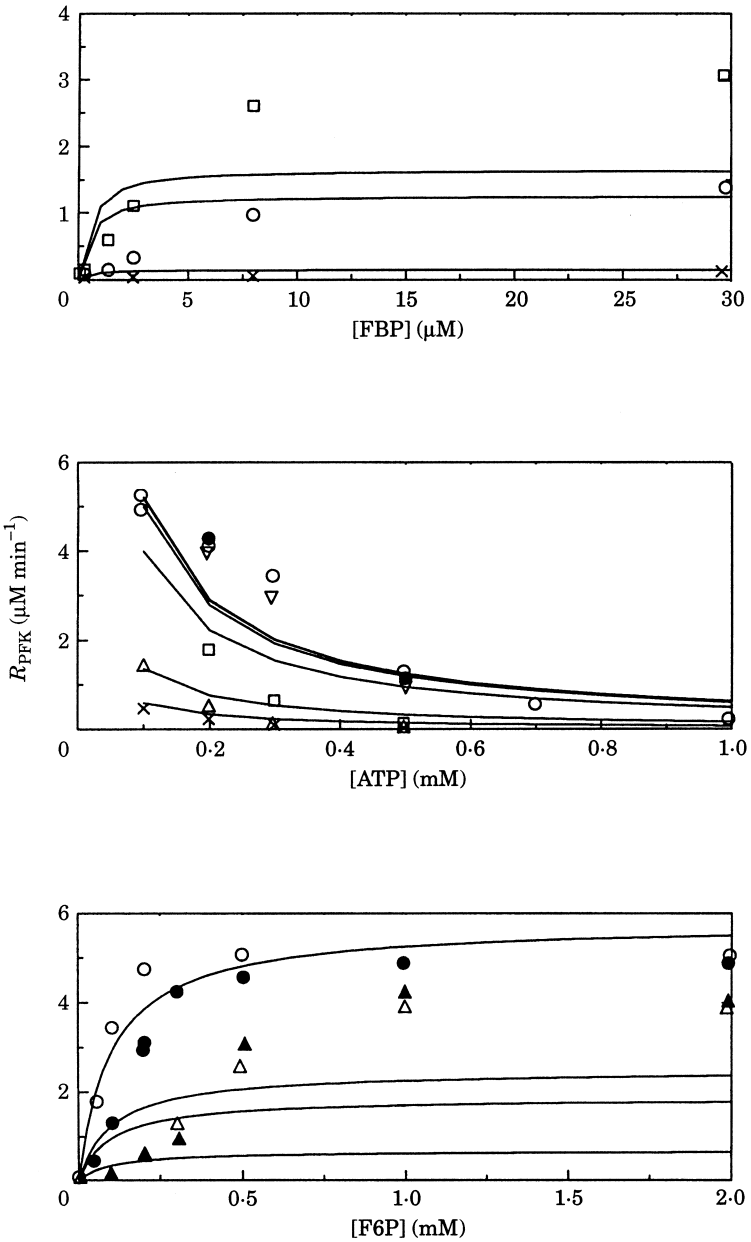

FIG. 1. PFK velocities calculated using the MWC model. Figures 1–3 Tornheim & Lowenstein (1976) are reproduced, top to bottom. Experimental points of Tornheim and Lowenstein are plotted with symbols corresponding to theirs; theoretical fits are plotted as smooth curves. Concentrations are given in the legend of Fig. 2. With ATP as substrate ligand 1, F6P ligand 2, FBP ligand 3, AMP ligand 4, and inhibitory ATP ligand 5; parameters for eqn (12) are: $L=3$, $k_T=k_R=110$ μM min^{-1}, $K_{1T}=K_{1R}=5$ μM, $K_{2T}=100$ μM, $K_{2R}=66.67$ μM, $K_{3T}=0.4$ μM, $K_{3R}=10$ μM, $K_{4T}=13.33$ μM, $K_{4R}=6.67$ μM, $K_{5T}=K_{5R}=20$ μM.

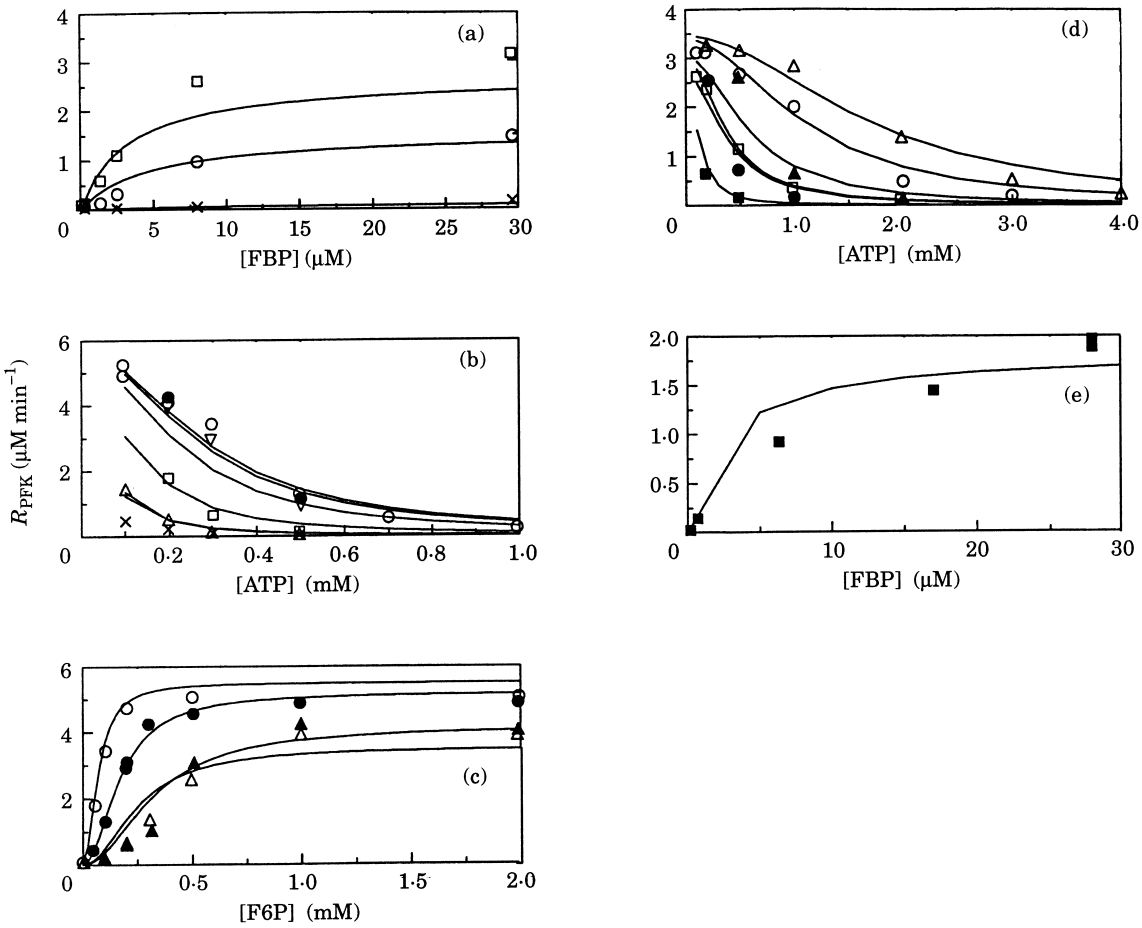

FIG. 2. The same PFK rates as in Fig. 1, calculated using the independent-subunit model. Figures 1–3 of Tornheim & Lowenstein (1976), with experimental data at pH 6.65, are reproduced in order in panels (a)–(c). Figures 4–5 of Tornheim & Lowenstein (1976), with experimental data at pH 7, are reproduced in order as panels (d)–(e). Experimental points are symbols, theoretical fits smooth curves. For pH 6.65 data, model parameters are: $V_{max} = 5.75$ μM min^{-1}, $\lambda = 0$, $f_{13} = 0.0829$, $f_{23} = 0.179$, $f_{41} = 3.44 \times 10^5$, $f_{42} = 2.45$, $f_{43} = 1.73 \times 10^6$, $f_{53} = 1.53 \times 10^4$, $K_1 = 7.12$ μM, $K_2 = 2.415$ μM, $K_3 = 70.3$ μM^2, $K_4 = K_5 = 1.2$ μM. For pH 7 data, parameters are: $V_{max} = 3.54$ μM min^{-1} ($\times 10$ for panel E), $\lambda = 0$, $f_{13} = 0.186$, $f_{23} = 0.0733$, $f_{41} = 125.7$, $f_{42} = 3.08$, $f_{43} = 2.56 \times 10^5$, $f_{53} = 6.22 \times 10^6$, $K_1 = 3.86$ μM, $K_2 = 0.8$ μM, $K_3 = 20.0$ (μM)^2, $K_4 = K_5 = 1.5$ μM. Ligand concentrations are: Panel (a), [ATP] = 0.5 mM, [F6P] = 0.1 mM, [FBP] varies, [AMP] = 50 μM (□), 20 μM (○), 1 μM for (×). Panel (b), [ATP] varies, [F6P] = 0.1 mM, [FBP] = 0.3 μM (△), 1.4 μM (□), 7.9 μM (▽), 32.0 μM (○), 84.0 μM (●), 0.3 μM (×). [AMP] = 20 μM except 1 μm (×). Panel (c), [ATP] = 0.1 mM (△) and (○), [F6P] varies, [FBP] = 32 μM except 1.4 μM (▲), [AMP] = 20 μM except 1 μM (△). Panel (d), [ATP] varies, [F6P] = 0.1 mM, [FBP] = 32 μM for open symbols and 0.3 μM for filled, [AMP] = 2 μM for squares, 20 μM for circles, 50 μM for triangles. Panel (e), [ATP] = 10 mM, [F6P] = 0.1 mM, [FBP] varies, [AMP] = 0.1 mM.

until the PFK rate equals *HK* again. But under these conditions the average GPDH rate also drops slightly, so [ATP] is dropping and [AMP] rising, and PFK is becoming more activated. Thus, [F6P] must drop by a large amount to give the requisite small decrease in the PFK rate. The power of [F6P] in the rate law does not affect this behavior.

This sensitivity can be alleviated by assuming some glucose-6-P dehydrogenase activity, or glucose-6-P phosphatase activity (the latter, however, has not been found in muscle). Also, product inhibition of hexokinase could make *HK* a decreasing function of [glucose-6-P]. Considering the rapid glucose-6-P—F6P equilibrium, any of these influences will keep [F6P] from becoming too large. As an example, take

$$R_{G6Pase} = k_{gp}[F6P] \tag{21}$$

and subtract this term from eqn (17) for d[F6P]/dt. Then the oscillatory solution shown in Fig. 3 is obtained. Concentrations, amplitudes, and period are similar to those in skeletal muscle extract (Tornheim, 1979).

The "G6Pase activity" required to achieve reasonable control is significant. Specifically, an average of 28% of F6P is lost via R_{G6Pase} under the conditions of Fig. 3, with the remainder going forward through

glycolysis. Also, the [ATP]/[ADP] ratio can become very high, oscillating between 2.8 and 83 (not shown). Oscillations exist over a very wide range of hexokinase rates HK, 0.9–64 μM min^{-1}. As HK is varied from 16 to 23 μM min^{-1}, the mean value of [F6P] doubles from 52 to 109 μM. The sensitivity of this mean value could be decreased further by increasing k_{gp}. The oscillations are not unduly sensitive to variations of other parameters.

There is a small λ assumed, corresponding to a "basal" PFK rate with F6P bound but AMP not bound, and/or FBP not bound, and/or inhibitory ATP bound. This rate must be finite to prevent [FBP] from tending toward zero, because otherwise, as [FBP] is decreased the rate of PFK decreases in an approximately first-order fashion, while that of GDPH (which consumes FBP) decreases only as the square root of [FBP].

The mechanism of oscillation can be described heuristically as follows: at the beginning ($t=0$ sec in Fig. 3) [FBP] is at a minimum, [F6P] is rising, and [ATP] is falling. The latter two changes both activate PFK so [FBP] begins to rise sharply and [F6P] passes through a maximum. Even as [F6P] falls, PFK continues to activate further as [FBP] rises. Here, it is evident that product activation of PFK by FBP is crucial for oscillations. However, then [ATP] begins to rise, and [AMP] as a consequence to fall. These two changes strongly inhibit PFK, as a result [FBP] falls and [F6P] rises. However, [ATP] remains at a high plateau for a considerable time, until [FBP] again reaches a minimum. Then the cycle repeats.

To visualize further the solution structure of a model such as this, it helps to simplify to two dependent variables. Then nullclines (curves where the derivative

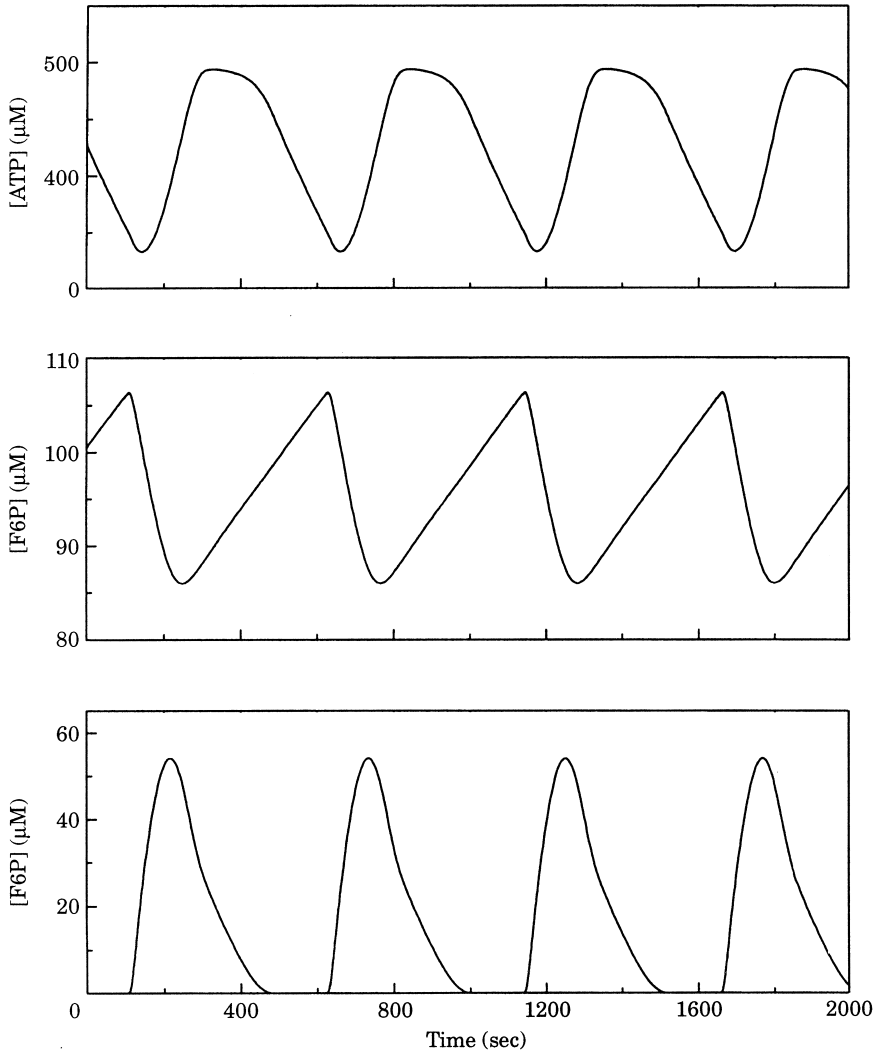

FIG. 3. Simulated glycolytic oscillations. PFK parameters are as in Fig. 2 with pH 6.65, except $\lambda=0.02$ and $V_{max}=108.0$ μM min^{-1}. Other parameters are: $A_{tot}=500$ μM, $K_A=1$, $HK=21.6$ μM min^{-1}, $K_{gf}=0.29$, $k_{ATP}=0.0576$ min^{-1}, $k_{GPDH}=12.6$ μM min^{-1}, $k_{gp}=0.0623$ min^{-1}, $K_D=8$ μM.

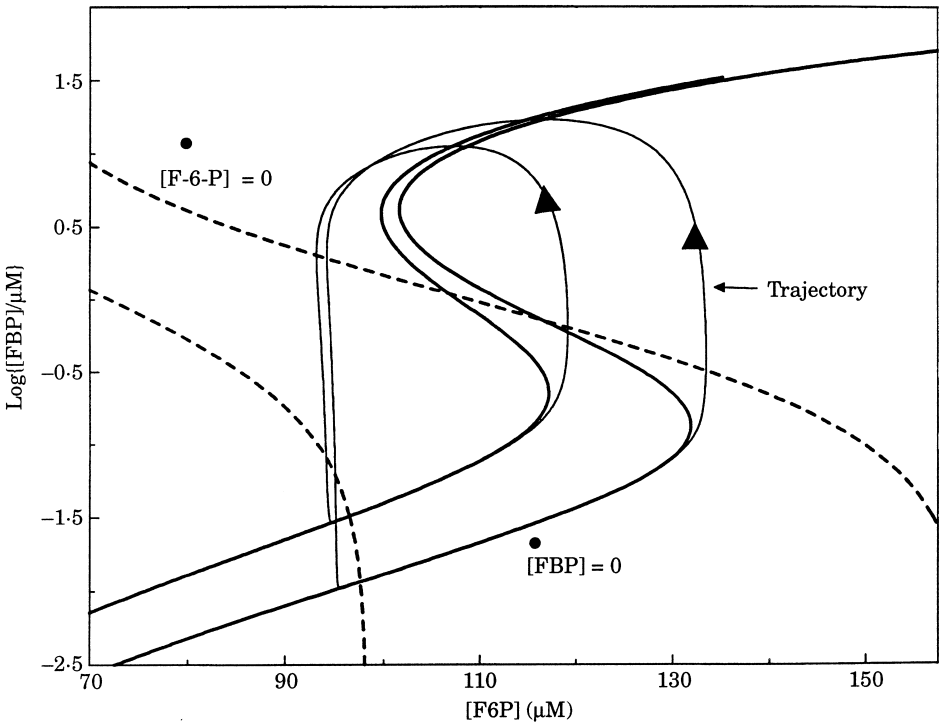

FIG. 4. Geometrical solution structure of the glycolytic oscillator with [ATP] fixed. Parameters as in Fig. 3 except [ATP] = 0.44 mM, $V_{max} = 1.08$ mM min^{-1}, and HK and λ vary. Along dashed [F6P] nullclines d[F6P]/d$t = 0$, $\lambda, = 0.4$, $HK = 72$ μM min^{-1} for the left nullcline and 126 μM min^{-1} for the other. Along heavy solid S-shaped [FBP] nullclines d[FBP]/d$t = 0$, $\lambda = 0.25$ for curve whose lower knee projects farther to the right and 0.4 for the other. For $HK = 126$ μM min^{-1} and $\lambda = 0.25$ or 0.4 trajectories are shown with arrows indicating direction of motion. For $HK = 72$ μM min^{-1} trajectories go to a stationary state at the intersection of the nullclines.

of one variable is zero) can be plotted in the plane of these variables. The trajectory always has a clear relationship to the nullclines. In the case of Fig. 3, the oscillations of all variables are significant, thus it is not mathematically evident that setting any one variable constant will give a system whose behavior resembles the original system. Nevertheless, it is found empirically that useful insights can be gained by examining the nullclines and trajectories of the two-variable system [eqns (17) and (18)] obtained by fixing [ATP]. Figure 4 shows two nullcline sets and trajectories for this system.

The [F6P] nullcline follows a curve of increasing [FBP] (more activation of PFK by its product) and decreasing [F6P] (more rapid utilization of F6P as a result of the increased product activation). The [FBP] nullcline forms an S-shaped curve when plotted against [F6P]. At low [F6P] the enzyme is very inactive and [FBP] is low, and at high [F6P], [FBP] is high. However, at intermediate [F6P] there exist two stable and one unstable steady states of PFK activity and consequently of [FBP], because of the activation of PFK by [FBP]. The existence of the bistable region depends on R_{GPDH} being proportional to a lesser power (the square root) of [FBP] than is R_{PFK}. The S shape is necessary for oscillations, and indeed oscillations occur when the [F6P] nullcline crosses *only* the unstable middle branch of the [FBP] nullcline. It is seen that increasing HK moves the [F6P] nullcline right and does not change the [FBP] nullcline. One sees that the mean values of both [F6P] and [FBP] increase. If HK is too high or too low, the system goes to a stationary state at the intersection of the [F6P] nullcline with the stable upper or lower branches of the [FBP] nullcline. Earlier, in modeling glycolytic oscillations in yeast, Venieratos & Goldbeter (1979), found similar behavior as the hexokinase rate was varied.

Figure 4 also shows that increasing λ raises the lower branch of the [FBP] nullcline and brings the right knee leftward. Then one sees that the amplitude of oscillations in [F6P] would be reduced, and also in [FBP], since the trajectory reaches the upper branch of the [FBP] nullcline more to the left. All these behaviors are qualitatively as seen in the full system. Finally, increasing V_{max} compresses both nullclines to the left and down (not shown) and thus is expected to preserve similar oscillations but at lower [F6P] and [FBP], which it does in the full system.

If parameters which fit the pH 7 PFK data are used, similar behavior to that above is obtained. Glycolytic

oscillations are again produced that are physiologically reasonable as regards period, amplitude, and mean concentrations (not shown). A high average [ATP]/[ADP] ratio is again maintained.

The final case considered is pH 7 PFK parameters with a total adenine nucleotide concentration of 10 mM and the differential equation for [ATP] changed to

$$\frac{d[ATP]}{dt} = -HK - R_{PFK} - R_{ATPase} + \frac{38}{2} R_{GPDH}. \quad (22)$$

This case is more representative of an intact cell, in which [ATP] is about 10 mM and in which, for each glucose molecule, approximately 38 ATP molecules are made and two used for phosphorylation, for a net yield of 36 ATP's per glucose. The model again predicts oscillations which appear physiologically reasonable, as shown in Fig. 5.

Again some glucose-6-phosphatase activity (or an analogous process) must be present to avoid undue sensitivity to HK. [ATP]/[ADP] varies from 3.5 to 182. Glycolytic parameters are not signficantly different from the extract simulation (Fig. 3) except that k_{ATP} is higher to balance the faster rate of ATP synthesis, and all other rate constants are similarly higher.

4. Discussion

A model for phosphofructokinase (PFK) kinetics has been constructed that is consistent with a considerable set of experimental rate data, and which is, in this repsect, a significant improvement over previous models. It is the first model based on mammalian PFK kinetics, and cannot be expected to apply to glycolytic oscillations dependent on, for example, yeast PFK kinetics. When combined with a model for the remainder of glycolytic pathway the model reproduces observed glycolytic rate and concentration oscillations in skeletal muscle extract rather well. The model can be simplified to two

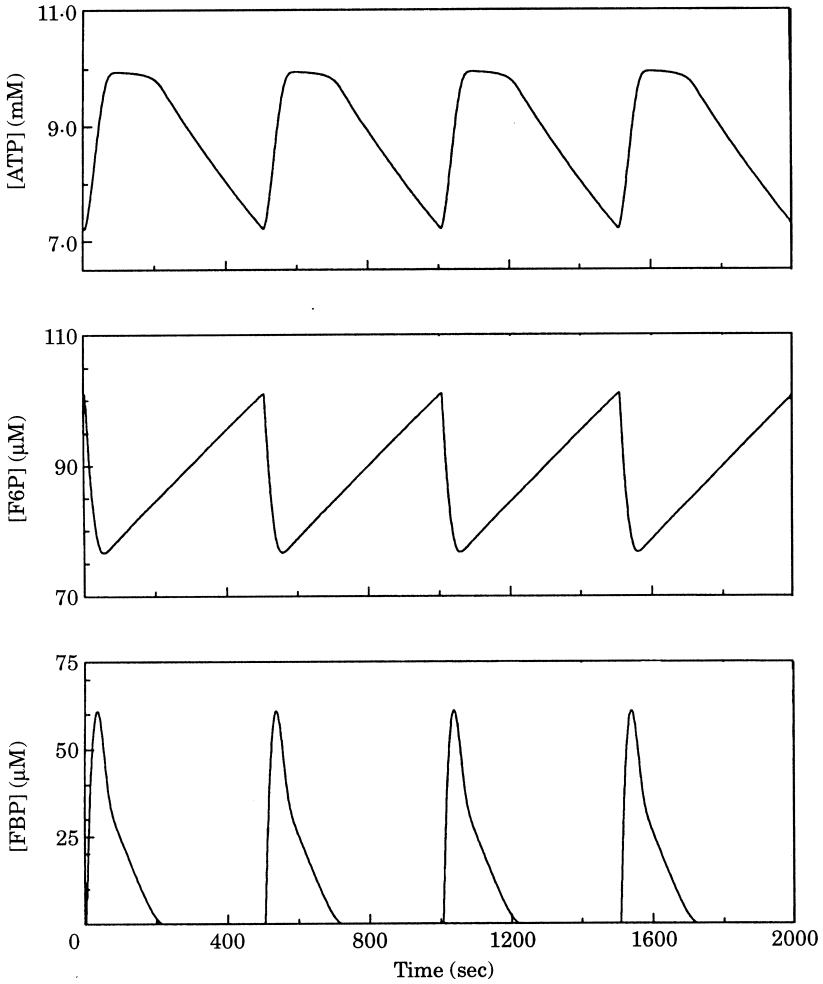

FIG. 5. Simulated glycolytic oscillations. PFK parameters as in Fig. 2 with pH 7, except $V_{max} = 900$ μM min^{-1}. Other parameters as in Fig. 3 except: $HK = 20.8$ μM min^{-1}, $k_{ATP} = 0.06$ min^{-1}, $k_{GPDH} = 30$ μM min^{-1}, $k_{gp} = 0.0667$ min^{-1}, $K_D = 200$ μM, $A_{tot} = 10.0$ mM.

dependent variables and analyzed in the phase plane to give a qualitative geometric intuition about the oscillation mechanism.

The model is not the type usually formulated for allosteric multisubunit enzymes such as PFK. However, an MWC model may not be appropriate for PFK kinetics, as evidenced by the following observations. Sigmoidicity of the velocity vs. [F6P] curve appears to require dilution of PFK and subsequent partial dissociation (Ramaiah & Tejwani, 1970; Donnicke *et al*., 1972; Bloxham & Lardy, 1975). Also, antibodies have been found that stabilize the aggregated, activated form of PFK against dilution or changes in buffer, and these antibodies also make the velocity vs [F6P] curve hyperbolic (Donnicke *et al*., 1972). Thus the most highly associated form of PFK appears to have the least sigmoidal kinetics, which is opposite to the prediction of an MWC model. Also, activation of muscle PFK by fructose 1,6-P_2 vs. fructose 2,6-P_2 is affected differently by other regulatory metabolites, suggesting there is more than one activated state of PFK (Tornheim, 1985), whereas a two-state MWC model has one activated and one relatively inactive state.

Nevertheless, attempts were made to fit the experimental data with an MWC model and an acceptable fit could not be obtained because that model could not account for the observed strong heterotropic interactions among ligands. It is possible that a very complex allosteric model, such as a sequential model of the type developed by (Koshland *et al*., 1966), could fit the PFK data because of the large number of states. However, such a model would be too algebraically complex to be readily intelligible.

The model constructed here, based on the assumption of identical independent subunits, includes interactions among ligands explicitly. [F6P] must enter the PFK rate expression squared to give sigmoidal curves of velocity vs. [F6P], and the model cannot mechanistically account for this dependence—some degree of cooperativity between subunits is likely to be responsible for the sigmoidicity. However, with present knowledge of PFK structure, the semi-empirical eqn (11) seems reasonable.

The oscillations found with PFK parameters that fit pH 6.65 data match well those found in skeletal muscle extract at this pH (Tornheim, 1979). The model predicts an extensive range of oscillations as glucose, and thus the hexokinase rate, is varied. There is one published observation of glycolytic oscillations at pH 7, with [ATP] about 10 mM, in the extract (Tornheim, 1988). Those oscillations in [ATP], [F6P], and [FBP] also are simulated well (Fig. 5) except for the experimentally observed decrease in ([ATP]+[ADP]+[AMP]) due to adenylate deaminase activity. In all the simulated oscillations a very high peak [ATP]/[ADP] ratio is reached. However, in skeletal muscle extract the peak [ATP]/[ADP] ratio is 25 or more with the total adenine nucleotide concentration near 0.5 mM (Tornheim, 1979), and in muscle *in vivo* the peak value as indicated by measured [creatine phosphate]/[creatine] ratios may be yet higher (Goodman & Lowenstein, 1977).

Also of interest is the fact that for stability of the model with respect to hexokinase rate variation, some glucose-6-P must be removed (or made less rapidly) at a rate increasing with its concentration. Removal of 28% or less suffices. Either glucose-6-phosphatase or glucose-6-P dehydrogenase may be postulated to provide this removal. The former enzyme has only been found in a few tissues, such as liver, and pancreatic β-cells (Chandramouli *et al*., 1991), but the latter is the first enzyme of the pentose phosphate pathway and is present in many tissues. The well-known product inhibition of hexokinase by glucose-6-P could also provide this stabilization.

The model of glycolysis used here can clearly be elaborated. Also, the assumption that ([ATP]+[ADP]+[AMP]) remains constant during oscillations is not borne out in experimental skeletal muscle extract (Tornheim & Lowenstein, 1973; Tornheim, 1979). To treat this matter would require modeling the kinetics of the purine nucleotide cycle, i.e. at least the reactions of the four enzymes adenylate deaminase, adenylosuccinate synthetase, adenylosuccinase, and myokinase. Recent skeletal muscle extract experiments (Tornheim, 1988; Andreas *et al*., 1990) Tornheim *et al*. (1991) have further explored the effects of citrate and fructose 2,6-P_2, and may allow refinement of the PFK model.

Of interest is the possibility that, in intact cells, glycolytic oscillations could be responsible for slow oscillations in the [ATP]/[ADP] ratio or related quantities such as the [NAD]/[NADH] ratio. Also, the cytoplasmic calcium concentration could be related to the [ATP]/[ADP] ratio through effects on ATP-dependent calcium pumps or, in excitable cells, through oscillations in the conductance of ATP-gated potassium channels and resultant oscillations in the membrane potential and in the activity of voltage-gated calcium channels. Most calcium oscillations reported in intact cells have periods of 1 min or less but there are a few examples (hepatocytes, endothelial cells, pancreatic acinar cells) in which periods of 2 min or more have been observed (Berridge & Galione, 1988). Perhaps glycolytic oscillations could underlie some slow calcium oscillations. Very recently there has been a report of oscillations of ATP-sensitive current and pyridine nucleotide levels in cardiac myocytes

(O'Rourke *et al*., 1994), which the authors suggest are due to glycolytic oscillations. Of particular interest is that in pancreatic β-cells in the islets of Langerhans, such calcium oscillations have been reported (Valdeolmillos *et al*., 1989; Gylfe *et al*., 1991), along with oscillations in oxygen consumption and insulin secretion (Longo *et al*., 1991), all with a period of around 5–20 min. Theoretical investigations (P. Smolen, unpublished) have identified glycolytic oscillations as a possible mechanism for explaining the oscillations in this cell type.

This work was initiated through discussions with Dr Joel Keizer and supported, in part, through NSF grant BIR 93-00799. I also acknowledge generous time and thought from Dr Keith Tornheim. I acknowledge computer time provided by the National Cancer Institute Biomedical Supercomputing Center.

REFERENCES

Andres, V., Schultz, V. & Tornheim, K. (1990). *J. biol. Chem.* **265,** 21441–21447.
Bar-Tana, J. & Cleland, W. (1974). *J. biol. Chem.* **249,** 1271–1280.
Berridge, M. & Galione, A. (1988). Faseb J. **2,** 3074–3082.
Bloxham, D. & Lardy, H. (1975). *The Enzymes*, 3rd edn (Boyer, P., ed.) Vol. VIII, pp. 239–278. New York: Academic Press.
Boiteaux, A., Goldbeter, A. & Hess, B. (1975). *Proc. natn. Acad. Sci. U.S.A.* **72,** 3829–3833.
Buckwitz, D., Jacobasch, G., Gerth, C., Holzhutter, H. & Thamm, R. (1988). *Mol. Bioch. Parasit.* **27,** 225–232.
Cantor, C. & Schimmel, P. (1980). *Biophysical Chemistry*, *Part III*, pp. 945–952. San Francisco: W. H. Freeman.
Chandramouli, V., Khan, A. Ostenson, C., Bergren, P., Low, H. Landau B. & Efendic, S. (1991). *Biochem. J.* **278,** 353–359.
Doedel, E. (1981). *Congr. Numer.* **30,** 265–284.
Donnicke, M. Hofer, H. & Pette, D. (1972). *FEBS Lett.* **20,** 184–186, 187–190.
Ermentrout, B. (1990). *PhasePlane*, *The Dynamical Systems Tool*. Pacific Grove, CA: Brooks-Cole Publishing Co.
Gear, C. (1967). *Math. Comp.* **21,** 146–156.
Goldbeter, A. & Lefever, R. (1972). *Biophys. J.* **12,** 1302-1315.
Goodman, M. & Lowenstein, J. (1977). *J. biol. Chem.* **252,** 5054–5060.
Gylfe, E. Grapengiesser, E. & Hellman, B. (1991). *Cell Calcium* **12,** 229–240.
Hanson, A., Rudolph, F. & Lardy, H. (1973). *J. biol. Chem.* **248,** 7852–7860.
Hess, B. & Boiteaux, A. (1971). *A. Rev. Biochem.* **40,** 237–258.
Hindmarsh, A. (1974). Report UCID-30001, Lawrence Livermore Laboratory.
IMSL (1991) *MathLibrary User's Manual*, *Version 2.0* pp. 981–986. Houston, TX: IMSL Customer Relations.
Kee, A. & Griffin, C. (1972). *Arch. Bioch. Biophys.* **149,** 361–370.
Kemp, R. & Krebs, E. (1967). *Biochemistry* **6,** 423–434.
Koppelschlager, G., Freyer, R., Diezel, W. & Hoffmann, E. (1968). *FEBS Lett.* **1,** 137–141.
Koshland, D., Nemethy, G. & Filmer, D. (1966). *Biochemistry* **5,** 365–385.
Ling, K. & Lardy, H. (1954). *J. Am. Chem. Soc.* **76,** 2842–2850.
Longo, E., Tornheim, K., Deeney, J., Varnum, B., Tillotson, D., Prentki, M. & Corkey, B. (1991). *J. biol. Chem.* **266,** 9314–9319.
Markus, M. & Hess, B. (1984). *Proc. natn. Acad. Sci. U.S.A.* **81,** 4394–4398.
Mathews, C. & Van Holde, K. (1990). *Biochemistry*, pp. 451–452. Redwood City, CA: Benjamin-Cummings.
Monod, J., Wyman, J. & Changeux, J. (1965). *J. molec. Biol.* **12,** 88–118.
O,Rourke, B., Ramza, B. & Marban, E. (1994). *Science* **265,** 962–966.
Parmeggiani, A. & Bowman, R. (1963). *Biochem. Biophys. Res. Commun.* **12,** 268–273.
Parmeggiani, A., Luft, J., Love, D & Krebs, E. (1966). *J. biol. Chem.* **241,** 4625–4637.
Passoneau, J. & Lowry, O. (1962). *Biochem. Biophys. Res. Commun.* **7,** 10–15.
Pettigrew, D. & Frieden, C. (1979). *J. biol. Chem.* **254,** 1896–1901.
Ramaiah, A. & Tejwani, G. (1970). *Biochem. Biophys. Res. Commun.* **39,** 1149–1156.
Richter, P. & Ross, J. (1981). *Science* **211,** 715–716.
Segel, I. (1975). *Enzyme Kinetics*, p. 646. New York: Wiley.
Termonia, Y. & Ross, J. (1981*a*). *Proc. natn. Acad. Sci. U.S.A.* **78,** 2952–2956.
Termonia, Y. & Ross, J. (1981*b*). *Proc. natn. Acad. Sci. U.S.A.* **78,** 3563–3566.
Tornheim, K. (1979). *J. theor. Biol.* **79,** 491–541.
Tornheim, K. (1985). *J. biol. Chem.* **260,** 7985–7989.
Tornheim, K. (1988). *J. biol. Chem.* **263,** 2619–2624.
Tornheim, K., Andres, V. & Schultz, V. (1991). *J. biol. Chem.* **266,** 15675–15678.
Tornehim, K. & Lowenstein, J. (1973). *J. biol. Chem.* **248,** 2670–2677.
Tornheim, K. & Lowenstein, J. (1975). *J. biol. Chem.* **250,** 6304–6314.
Tornheim, K. & Lowenstein, J. (1976). *J. biol. Chem.* **251,** 7322–7328.
Uyeda, K. (1991). In: *A Study of Enzymes*, *Vol. 2* (Kuby, S., ed.) pp. 445–456. Boca Raton, FL: CRC Press.
Uyeda, K. & Racker, E. (1965). *J. biol. Chem.* **240,** 4682–4693.
Valdeolmillos, M., Santos, R., Contreras, D., Soria, B. & Rosario, L. (1989). *FEBS Lett.* **259,** 19–23.
Venieratos, D. & Goldbeter, A. (1979). *Biochimie* **61,** 1247–1256.
Waser, M., Garfinkel, L., Kohn, M. & Garfinkel D. (1983). *J. theor. Biol.* **103,** 295–312.